JOURNAL OF GUIDANCE, CONTROL, AND DYNAMICS
Vol. 27, No. 5, September–October 2004

Adaptive Linear Parameter Varying Control Synthesis for Actuator Failure

Jong-Yeob Shin*
National Institute of Aerospace, Hampton, Virginia 23666
N. Eva Wu†
Binghamton University, Binghamton, New York 13902
and
Christine Belcastro‡
NASA Langley Research Center, Hampton, Virginia 23681

A robust linear parameter varying (LPV) control synthesis is carried out for a Highly Maneuverable Aircraft Technology (HiMAT) vehicle subject to loss of control effectiveness. The scheduling parameter is selected to be a function of the estimates of the control effectiveness factors. The estimates are provided online by a two-stage adaptive Kalman filter estimator. The inherent conservatism of the LPV design is reduced through the use of a scaling factor on the uncertainty block that represents the estimation errors of the effectiveness factors. Simulations of the controlled system with the online estimator show that a superior fault tolerance can be achieved.

Introduction

ONE of the most effective methods for achieving single aircraft accident prevention[1] is to design flight control laws that are fault tolerant. An active fault-tolerant control (FTC) system requires its control law to react to actuator/sensor faults through reconfiguration. It is important that the design of a fault detection and isolation (FDI) mechanism in an FTC system be properly integrated with the design of an FTC mechanism.[2]

FTC designs for aerospace vehicles based on linear matrix inequality (LMI) optimization solutions can be found in several reports. For example, in Refs. 3 and 4, fault-tolerant controllers are designed based on the information provided by separate FDI modules that are assumed to have been identified faults, whereas faults are modeled as functions of model parameters. In particular, when faults are modeled as a set of varying parameters in a linear parameter varying (LPV) system, a known LPV control synthesis method[5,6] could be applied. The synthesis is formulated into an LMI optimization problem based on the LPV system whose state-space matrices are functions of a scheduling parameter vector. A scheduling parameter vector must be measurable in real time, and its rate of change is required to be bounded.[5,6] It is possible that an LPV controller can robustly stabilize a closed-loop system and achieve a desired performance level over the entire parameter space. The LPV synthesis methodology has been successfully applied to synthesize controllers for pitch-axis missile autopilots,[7,8] F-14 aircraft lateral–directional axis,[9] turbofan engines,[10] and F-16 aircraft.[11]

In this paper, fault parameters are considered as scheduling parameters in LPV control synthesis, whose rate of change is sufficiently large but not infinite. In practice, the bounded large number of a scheduling parameter rate of change can allow abrupt fault occurrence in a reconfigurable LPV controller.[4] The fault parameters can be provided by separate FDI modules. The main contribution of this paper is the integration of FTC design with an FDI module. The fault parameters are estimated online using a two-stage adaptive Kalman filtering scheme (see Ref. 12). Modeling fault parameter estimation error is also included as the part of a control synthesis problem formulation. This estimation error enters in the construction of an LPV controller in the form of an uncertainty block. Thus the online parameter estimator can be integrated into the LPV controller in an FTC system. The LPV control synthesis problem can be formulated as a robust LPV control synthesis.[5,13] The robust LPV control synthesis problem is translated into two LMI optimization problems to relax the constraints of fixing a controller in the iteration procedure.

A system with two actuators that can fail one at a time is considered. Thus, the reconfigurability of the system never goes to zero. More specifically, an LPV model is established that captures two actuator failures in a single scheduling parameter that is a function of the two actuator effectiveness factors[12] to reduce unnecessary conservativeness. The factors are estimated using a two-stage adaptive Kalman filter. A set of covariance-dependent forgetting factors is introduced into the filtering algorithm.[12] As a result, the change in the actuator effectiveness is accentuated to help achieve a more accurate estimate more rapidly. The H_∞ bounds on parameter estimation errors are assessed through simulations, which are then used as bounds of real parameter uncertainty in the construction of a robust LPV control law. Therefore, a fault-tolerant control design is equated to an LPV control synthesis using online estimated fault parameters.

This paper contains the following sections. In the second section, a robust LPV synthesis method is described. In the third section, a fault parameter estimation method is presented. In the fourth section, an LPV controller for a Highly Maneuverable Aircraft Technology (HiMAT) vehicle is designed using the robust LPV synthesis control method. In the fifth section, simulation results of the closed-loop HiMAT vehicle with a robust LPV control law and an online estimator are presented. This paper is concluded with a brief summary of our findings in the sixth section.

Robust LPV Control Synthesis

This section states the general problem of control synthesis that concerns an uncertain LPV system, describes a control synthesis procedure, and introduces an estimator for actuator effectiveness. Therefore, the synthesis of a control law is specialized to tolerating the reduction of actuator effectiveness,[12] which reflects the severity of some actuator and control surface failure cases. The estimated effectiveness factors are identified with a subset of varying parameters, and the estimation errors are identified with real parameter uncertainties.

Received 26 August 2002; accepted for publication 8 March 2004.

*Staff Scientist. Member AIAA.
†Professor, Department of Electrical and Computer Engineering.
‡Researcher, Guidance Control Branch.

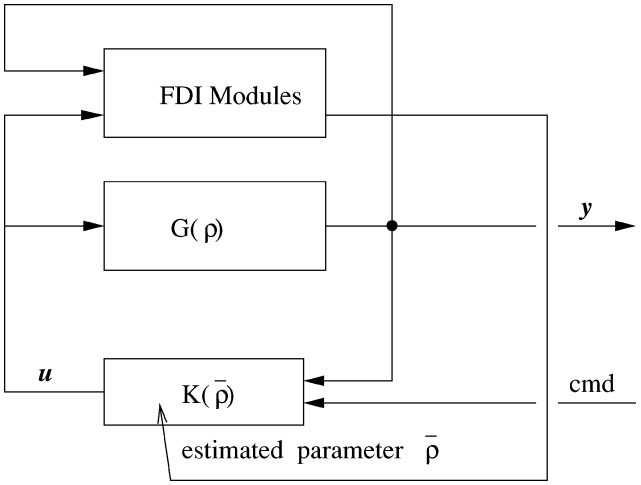

Fig. 1 General FTC system structure.

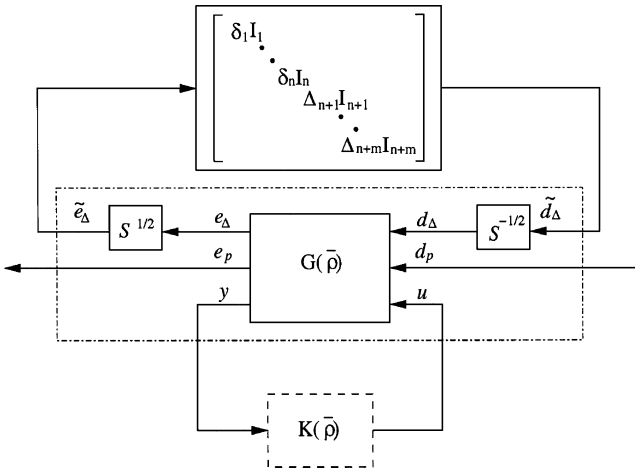

Fig. 2 General augmented LPV open-loop system inside the dashed-dotted box with the interconnection of the uncertainty block and a controller $K(\bar{\rho})$.

Robust Control Problem for an Uncertain LPV Plant

Suppose the dynamics of a plant can be modeled as an LPV system for which fault occurrence can be described by a function of scheduling parameters $\rho(t)$ such that $\rho(t) \in \mathcal{F}_\rho$ where $\mathcal{F}_\rho$ is a compact set in the n-dimensional real space $\mathcal{R}^n$. These parameters cannot be directly measured but can be estimated online with bounded estimation errors by an FDI module. Our goal is to design an FTC law that is adaptive to the change of the estimated fault parameter $\bar{\rho}(t)$. The proposed structure of an FTC system is shown in Fig. 1 including an FDI module, an open-loop system $G(\rho)$, and a controller $K(\bar{\rho})$. Note that an open-loop system is a function of scheduling parameters and that a controller is a function of the estimated parameters.

Assume that the estimation errors by the FDI module in Fig. 1 are bounded, that is,

$$|\rho(t) - \bar{\rho}(t)| \le \delta_{\bar{\rho}}, \qquad \delta_{\bar{\rho}} \in \mathcal{R} \tag{1}$$

Also, assume that the state-space matrices of the open-loop system $G(\rho)$ are rational or affine with respect to parameters ρ. Then the open-loop system can be expressed in an upper linear fraction transformation (LFT) form with respect to the estimation errors,[14]

$$G(\bar{\rho}(t) \pm \delta_{\bar{\rho}}) = F_u[G(\bar{\rho}), \Delta_\rho] \tag{2}$$

where F_u is the upper LFT and Δ_ρ is estimation errors such that

$$\Delta_\rho = \mathrm{diag}(\delta_1 I_1, \ldots, \delta_n I_n) \tag{3}$$

with n the number of the estimated parameters. The reader is referred to Refs. 14 and 15 for the definition of the upper LFT and the LFT formulation for a system in polynomial functions.

The LFT representation in Eq. (2) for the LPV system will be called an LFT–LPV system and can be written in the following general form. Consider an open-loop system as an LFT–LPV system,

$$\begin{bmatrix} \dot{\boldsymbol{x}} \\ \boldsymbol{e}_\Delta \\ \boldsymbol{e}_p \\ \boldsymbol{y} \end{bmatrix} = \begin{bmatrix} A(\bar{\rho}) & B_\Delta(\bar{\rho}) & B_p(\bar{\rho}) & B_u(\bar{\rho}) \\ C_e(\bar{\rho}) & D_{\Delta\Delta}(\bar{\rho}) & D_{\Delta p}(\bar{\rho}) & D_{\Delta u}(\bar{\rho}) \\ C_p(\bar{\rho}) & D_{p\Delta}(\bar{\rho}) & D_{pp}(\bar{\rho}) & D_{pu}(\bar{\rho}) \\ C_y(\bar{\rho}) & D_{y\Delta}(\bar{\rho}) & D_{yp}(\bar{\rho}) & 0 \end{bmatrix} \begin{bmatrix} \boldsymbol{x} \\ \boldsymbol{d}_\Delta \\ \boldsymbol{d}_p \\ \boldsymbol{u} \end{bmatrix} \tag{4}$$

$$\boldsymbol{d}_\Delta = \Delta \boldsymbol{e}_\Delta \tag{5}$$

where state $\boldsymbol{x} \in \mathcal{R}^{n_x}$, control input $\boldsymbol{u} \in \mathcal{R}^{n_u}$, and measured output $\boldsymbol{y} \in \mathcal{R}^{n_y}$. Disturbance and errors are represented by $\boldsymbol{d}_p \in \mathcal{R}^{n_d}$ and $\boldsymbol{e}_p \in \mathcal{R}^{n_e}$. Signals $\boldsymbol{e}_\Delta \in \mathcal{R}^{n_\Delta}$ and $\boldsymbol{d}_\Delta \in \mathcal{R}^{n_\Delta}$ are associated with the uncertainty matrix Δ in Eq. (5). All of the state-space matrices are of appropriate dimensions.

The uncertainty matrix Δ is in a structured uncertainty block set Δ,

$$\Delta = \Big\{ \Delta = \mathrm{diag}(\delta_1 I_1, \ldots, \delta_n I_n, \Delta_{n+1}, \ldots, \Delta_{n+m}) : \delta_i \in R, \Delta_i \in C^{l \times l}, \bar{\sigma}(\Delta) \le \beta \Big\} \tag{6}$$

where β is normalized to 1 without loss of generality. Here, δ_i and Δ_i represent estimation errors δ_ρ and uncertainties associated with unmodeled dynamics, respectively.

Now, the conventional LPV synthesis methodology[6,9,16] can be applied for the design of an LPV controller for the open-loop system. The methodology in Refs. 6 and 16, however, leads to conservative results in performance because it does not use structural information on the uncertainty block relating the input and output signals. To reduce the conservativeness in LPV synthesis, a scaling matrix S is introduced in Refs. 5 and 13. The scaling matrix S over the uncertainty block relating the input and output signals belongs to a set $\boldsymbol{S}_\Delta$,

$$\boldsymbol{S}_\Delta = \{ S : S > 0, S\Delta = \Delta S, S \in \mathcal{R}^{n_\Delta \times n_\Delta}, \Delta \in \boldsymbol{\Delta} \} \tag{7}$$

Thus, the mapping Δ from $\boldsymbol{e}_\Delta$ to $\boldsymbol{d}_\Delta$ with scaling matrix S (Fig. 2) remains the same as Eq. (5). The interconnection block diagram with an open-loop system, an uncertainty block Δ, a scaling matrix S, and an LPV controller $K(\bar{\rho})$ is shown in Fig. 2.

Now, the robust LPV control synthesis problem can be stated as designing an LPV controller $K(\bar{\rho})$ with a scaling matrix S that minimizes the induced-$\mathcal{L}_2$ norm of the closed-loop LPV system,[11] that is,

$$\min_{K(\bar{\rho}), S \in \boldsymbol{S}_\Delta} \left\| \begin{bmatrix} S^{\frac{1}{2}} & 0 \\ 0 & I \end{bmatrix} F_l[G(\bar{\rho}), K(\bar{\rho})] \begin{bmatrix} S^{-\frac{1}{2}} & 0 \\ 0 & I \end{bmatrix} \right\|_{2 \leftarrow 2} \tag{8}$$

where the lower LFT $F_l[G(\bar{\rho}), K(\bar{\rho})]$ represents the closed-loop system with the controller $K(\bar{\rho})$ in Ref. 15. The optimization problem of Eq. (8) is not convex in $K(\bar{\rho})$ and S. Note that the problem of Eq. (8) is similar to a D–K iteration problem in Ref. 15, when estimated scheduling parameters $\bar{\rho}$ are fixed. A D–K iteration is for a linear time-invariant system with a scaling matrix D, which is calculated in the frequency domain. In general, the iteration number in a D–K iteration increases a designed control state order. The optimization problem of Eq. (8) is for an uncertain LPV system, and a scaling matrix S is calculated in the time domain. In the optimization problem, a designed control state order does not change as a scaling matrix S. The following section describes a reformulation of the problem so that it can be solved via an iterative procedure.

Control Synthesis Methodology

In this subsection, an iterative procedure of solving the optimization problem of Eq. (8) is presented. Hereafter, $\bar{\rho}$ is suppressed in the $\bar{\rho}$-dependent matrices. Suppose a scaling matrix S is given. The augmented LPV open-loop system shown as a dash-dotted box in

Fig. 2 with the scaling matrix S can be written as

$$\begin{bmatrix} \dot{\boldsymbol{x}} \\ \tilde{\boldsymbol{e}}_\Delta \\ \boldsymbol{e}_p \\ \boldsymbol{y} \end{bmatrix} = \begin{bmatrix} A & B_\Delta S^{-\frac{1}{2}} & B_p & B_u \\ S^{\frac{1}{2}} C_e & S^{\frac{1}{2}} D_{\Delta\Delta} S^{-\frac{1}{2}} & S^{\frac{1}{2}} D_{\Delta p} & S^{\frac{1}{2}} D_{\Delta u} \\ C_p & D_{p\Delta} S^{-\frac{1}{2}} & D_{pp} & D_{pu} \\ C_y & D_{y\Delta} S^{-\frac{1}{2}} & D_{yp} & 0 \end{bmatrix} \begin{bmatrix} \boldsymbol{x} \\ \tilde{\boldsymbol{d}}_\Delta \\ \boldsymbol{d}_p \\ \boldsymbol{u} \end{bmatrix} \tag{9}$$

$$\begin{bmatrix} M_{11} & PB_{1_{\rm cl}} + \gamma_s^{-1} C_{2_{\rm cl}}^T D_{21_{\rm cl}} + C_{1_{\rm cl}}^T S D_{11_{\rm cl}} & PB_{2_{\rm cl}} + \gamma_s^{-1} C_{2_{\rm cl}}^T D_{22_{\rm cl}} + C_{1_{\rm cl}}^T S D_{12_{\rm cl}} \\ \star & \gamma_s^{-1} D_{21_{\rm cl}}^T D_{21_{\rm cl}} + D_{11_{\rm cl}}^T S D_{11_{\rm cl}} - S & \gamma_s^{-1} D_{21_{\rm cl}}^T D_{22_{\rm cl}} + D_{11_{\rm cl}}^T S D_{12_{\rm cl}} \\ \star & \star & \gamma_s^{-1} D_{22_{\rm cl}}^T D_{22_{\rm cl}} + D_{12_{\rm cl}}^T S D_{12_{\rm cl}} - I \end{bmatrix} < 0 \tag{18}$$

The LPV control synthesis methodology in Refs. 6 and 16 can be applied for the augmented open-loop system under the assumptions that

$$\begin{bmatrix} S^{\frac{1}{2}} D_\Delta \\ \Delta_{pu} \end{bmatrix}$$

is of full column rank for all $\bar{\rho}(t)$ and $[\Delta_{y\Delta} S^{-1/2} \;\; D_{yp}]$ is of full row rank for all $\bar{\rho}(t)$.

For the sake of completeness, a brief summary of the LPV control synthesis methodology in Ref. 6 is given in this section. In Ref. 6, an LPV control synthesis is formulated into an LMI optimization such that the closed-loop system achieves exponential stability and an induced-$\mathcal{L}_2$ norm of disturbance signals to error signals is minimized. The LMI optimization is

$$\min_{0 < X(\bar{\rho}), 0 < Y(\bar{\rho})} \gamma \tag{10}$$

subject to the LMI constraints defined in Ref. 6. The designed LPV controller $K(\bar{\rho})$ is written as

$$\begin{bmatrix} \dot{x}_k \\ u \end{bmatrix} = \begin{bmatrix} A_k(\bar{\rho}) & B_k(\bar{\rho}) \\ C_k(\bar{\rho}) & D_k(\bar{\rho}) \end{bmatrix} \begin{bmatrix} x_k \\ y \end{bmatrix} \tag{11}$$

where the realization of control matrices $A_k(\bar{\rho})$, $B_k(\bar{\rho})$, $C_k(\bar{\rho})$, and $D_k(\bar{\rho})$ from the solution matrices $X(\bar{\rho})$ and $Y(\bar{\rho})$ in Eq. (10) follows that from Ref. 6.

Suppose an designed LPV controller $K(\bar{\rho})$ in Eq. (11) is given. The closed-loop LPV system with the controller is

$$\begin{bmatrix} \dot{\boldsymbol{x}}_{\rm cl} \\ \tilde{\boldsymbol{e}}_\Delta \\ \boldsymbol{e}_p \end{bmatrix} = \begin{bmatrix} A_{\rm cl} & B_{1_{\rm cl}} S^{-\frac{1}{2}} & B_{2_{\rm cl}} \\ S^{\frac{1}{2}} C_{1_{\rm cl}} & S^{\frac{1}{2}} D_{11_{\rm cl}} S^{-\frac{1}{2}} & S^{\frac{1}{2}} D_{21_{\rm cl}} \\ C_{2_{\rm cl}} & D_{21_{\rm cl}} S^{-\frac{1}{2}} & D_{22_{\rm cl}} \end{bmatrix} \begin{bmatrix} \boldsymbol{x}_{\rm cl} \\ \tilde{\boldsymbol{d}}_\Delta \\ \boldsymbol{d}_p \end{bmatrix} \tag{12}$$

where $\boldsymbol{x}_{\rm cl}^T = [\boldsymbol{x}^T \;\; \boldsymbol{x}_k^T]$,

$$A_{\rm cl} = \begin{bmatrix} A + B_u D_k C_y & B_u C_k \\ B_k C_y & A_k \end{bmatrix} \tag{13}$$

$$[B_{1_{\rm cl}} \quad B_{2_{\rm cl}}] = \begin{bmatrix} B_\Delta & B_p \\ 0 & 0 \end{bmatrix} + \begin{bmatrix} B_u D_k & B_u D_k \\ B_k & B_k \end{bmatrix} \begin{bmatrix} D_{y\Delta} & 0 \\ 0 & D_{yp} \end{bmatrix} \tag{14}$$

$$\begin{bmatrix} C_{1_{\rm cl}} \\ C_{2_{\rm cl}} \end{bmatrix} = \begin{bmatrix} C_e + D_{\Delta u} D_k C_y & D_{\Delta u} C_k \\ C_p + D_{pu} D_k C_y & D_{pu} C_k \end{bmatrix} \tag{15}$$

$$\begin{bmatrix} D_{11_{\rm cl}} & D_{12_{\rm cl}} \\ D_{21_{\rm cl}} & D_{22_{\rm cl}} \end{bmatrix} = \begin{bmatrix} D_{\Delta\Delta} & D_{\Delta p} \\ D_{p\Delta} & D_{pp} \end{bmatrix} + \begin{bmatrix} D_{\Delta u} \\ D_{pu} \end{bmatrix} D_k [D_{y\Delta} \quad D_{yp}] \tag{16}$$

Applying the Kalman–Yakubovich–Popov lemma (see Ref. 17), the following LMI optimization problem is formulated for finding a scaling factor S that leads to minimization of an induced-$\mathcal{L}_2$ norm of the closed-loop system:

$$\min_{P > 0, S \in S_\Delta} \gamma_s \tag{17}$$

subject to

where

$$M_{11} = A_{\rm cl}^T P + P A_{\rm cl} + \dot{P} + \gamma_s^{-1} C_{2_{\rm cl}}^T C_{2_{\rm cl}} + C_{1_{\rm cl}}^T S C_{1_{\rm cl}}$$

and $\star$ represents the symmetric component of the LMI constraint in Eq. (18).

Now, the problem in Eq. (8) can be solved using the following iteration procedure.

1) Design an LPV controller $K(\bar{\rho})$ for an augmented open-loop system with a scaling matrix S by solving the LMI optimization in Eq. (10). At the first iteration, S is assumed to be the identity matrix I.

2) Generate the closed-loop system with the designed LPV controller and solve the LMI optimization problem in Eq. (17) to find a scaling matrix S.

3) Generate an augmented open-loop system with the scaling matrix S using Eq. (9).

4) Iterate over steps 1–3 until convergence, or terminate the iteration on satisfaction with a designed LPV controller.

This proposed iteration method is one of the possible methodologies to solve the robust LPV problem in Eq. (8). Note that this iteration method can not guarantee finding global solutions of K and S because the problem in Eq. (8) is not convex in K and S. Also, there is no guarantee of convergence in the iteration process. This iteration procedure is, however, practically tractable to synthesize an LPV controller and to calculate a scaling matrix.

Reported research results[5,13] on robust LPV synthesis are few. In Ref. 5, an iteration procedure is suggested by using scaling matrix S, which is similar to the iteration method described in this section. The suggested LMI problems in Ref. 5, however, have an algebraic constraint that is hard to satisfy in practice. In Ref. 13, the robust LPV synthesis problem is formulated as a bilinear matrix inequality problem, which also requires iterations to solve the problem including an algebraic constraint. Note that the iteration method described in this section does not have an algebraic constraint. Also, in the iteration method, the matrix $P(\bar{\rho})$ is free (not fixed) when a scaling matrix S is calculated in step 2. This leads to relaxation of the constraints of fixing the LPV controller $K(\bar{\rho})$.

Parameter Estimation

This section briefly describes the formulation of an actuator effectiveness estimation problem, which makes it possible to transform an FTC (loss of actuator effectiveness) problem to a robust LPV control problem. The development of this section follows that in Ref. 12.

Consider a linear discrete model as

$$\boldsymbol{x}_{k+1} = A_k^d \boldsymbol{x}_k + B_k^d \boldsymbol{u}_k, \qquad \boldsymbol{y}_{k+1} = C_k \boldsymbol{x}_{k+1} \tag{19}$$

where $\boldsymbol{x}_k \in \mathcal{R}^{n_x}$, $\boldsymbol{u}_k \in \mathcal{R}^{n_u}$, and $\boldsymbol{y}_k \in \mathcal{R}^{n_y}$ are the state, input, and output variables, respectively. The discrete matrices A_k^d and B_k^d can be obtained from a continuous model via, for example, Euler's rule with a sampling period T_s.

To include the possible loss of control effectiveness in the model, n_u control effectiveness factors $-1 \le \xi_k^j \le 0$, $j = 1, \ldots, n_u$, are

introduced as functions of discrete time k. For effectiveness factor estimation, the linear discrete design model is rewritten as

$$\boldsymbol{x}_{k+1} = A_k^d \boldsymbol{x}_k + \begin{bmatrix} b_1^d \boldsymbol{\xi}_k^1 & \cdots & b_{n_u}^d \boldsymbol{\xi}_k^{n_u} \end{bmatrix} \begin{bmatrix} \boldsymbol{u}_k^1 \\ \boldsymbol{u}_k^2 \\ \vdots \\ \boldsymbol{u}_k^{n_u} \end{bmatrix} + B_k^d \boldsymbol{u}_k + w_k^x \quad (20)$$

$$= A_k^d \boldsymbol{x}_k + E_k^d \boldsymbol{\xi}_k + B_k^d \boldsymbol{u}_k + w_k^x \quad (21)$$

$$\boldsymbol{\xi}_{k+1} = \boldsymbol{\xi}_k + w_k^{\xi} \quad (22)$$

$$\boldsymbol{y}_k = C_k^d x_k + v_k \quad (23)$$

where the effectiveness factor vector $\boldsymbol{\xi}_k$ is defined as $[\boldsymbol{\xi}_k^1 \ \cdots \ \boldsymbol{\xi}_k^{n_u}]^T$. It is obvious that $E_k^d = B_k^d \times \text{diag}\{\boldsymbol{u}_k^1, \ldots, \boldsymbol{u}_k^{n_u}\}$. Here w_k^x, w_k^{ξ}, and v_k are the white noise sequences of uncorrelated Gaussian random vectors with zero means and covariance matrices Q_k^x, Q_k^{ξ}, and R_k, respectively.

The minimum variance solution is obtained by a direct application of the two-stage Kalman filter algorithm of Keller and Darouach,[18] with constant coefficient matrices in Ref. 18 replaced by time-varying matrices. In this paper, the compensated state and error covariance estimation step in Ref. 18 is not used because it is not related with control effectiveness factor estimates $\hat{\boldsymbol{\xi}}_{k+1|k+1}$ in the filter. The filter algorithm used in this paper is decoupled into three sets of equations.

Optimal effectiveness factor estimator:

$$\hat{\boldsymbol{\xi}}_{k+1|k} = \hat{\boldsymbol{\xi}}_{k|k} \quad (24)$$

$$P_{k+1|k}^{\xi} = P_{k|k}^{\xi} + Q_k^{\xi} \quad (25)$$

$$K_{k+1}^{\xi} = P_{k+1|k}^{\xi} H_{k+1|k}^T \left(H_{k+1|k} P_{k+1|k}^{\xi} H_{k+1|k}^T + \tilde{S}_{k+1} \right)^{-1} \quad (26)$$

$$P_{k+1|k+1}^{\xi} = \left(I - K_{k+1}^{\xi} H_{k+1|k} \right) P_{k+1|k}^{\xi} \quad (27)$$

$$\hat{\boldsymbol{\xi}}_{k+1|k+1} = \hat{\boldsymbol{\xi}}_{k+1|k} + K_{k+1}^{\xi} (\tilde{r}_{k+1} - H_{k+1|k} \hat{\boldsymbol{\xi}}_{k|k}) \quad (28)$$

State estimator:

$$\tilde{\boldsymbol{x}}_{k+1|k} = A_k^d \tilde{\boldsymbol{x}}_{k|k} + B_k^d \boldsymbol{u}_k + W_k \hat{\boldsymbol{\xi}}_{k|k} - V_{k+1|k} \hat{\boldsymbol{\xi}}_{k|k} \quad (29)$$

$$\tilde{P}_{k+1|k}^x = A_k^d \tilde{P}_{k|k}^x \left(A_k^d \right)^T + Q_k^x + W_k P_{k|k}^{\xi} W_k^T - V_{k+1|k} P_{k+1|k}^{\xi} V_{k+1|k}^T \quad (30)$$

$$\tilde{K}_{k+1}^x = \tilde{P}_{k+1|k}^x \left(C_{k+1}^d \right)^T \left\{ C_{k+1}^d \tilde{P}_{k+1|k}^x \left(C_{k+1}^d \right)^T + R_{k+1} \right\}^{-1} \quad (31)$$

where the filter residual and its covariance are given as

$$\tilde{r}_{k+1} = \boldsymbol{y}_{k+1} - C_{k+1}^d \tilde{\boldsymbol{x}}_{k+1|k} \quad (32)$$

$$\tilde{S}_{k+1} = C_{k+1}^d \tilde{P}_{k+1|k}^x \left(C_{k+1}^d \right)^T + R_{k+1} \quad (33)$$

Coupling equations:

$$W_k = A_k^d V_{k|k} + E_k^d \quad (34)$$

$$V_{k+1|k} = W_k P_{k|k}^{\xi} \left(P_{k+1|k}^{\xi} \right)^{-1} \quad (35)$$

$$H_{k+1|k} = C_{k+1}^d V_{k+1|k} \quad (36)$$

$$V_{k+1|k+1} = V_{k+1|k} - \tilde{K}_{k+1}^x H_{k+1|k} \quad (37)$$

The variable definitions are taken from Ref. 18. A further measure is taken to modify the preceding filtering algorithm so that the estimates become more responsive to abrupt changes in the control effectiveness factors.

A well-known technique for estimating time-varying parameters is the use of forgetting factors. The basic idea is to enable a recursive algorithm to discount the past information so that the filter is more apt to recognize the changes in the system. Because the time update of the factor estimate governed by Eq. (24) is the dominant opposing force to acknowledge the abrupt changes in the effectiveness factors, forgetting factors introduced into the time propagation of the covariance $P_{k|k}^{\xi}$ in Eq. (25) are likely to function most effectively.

Assume that the covariance $P_{k|k}^{\xi}$ adequately describes the effectiveness factor estimation error along both temporal and spatial directions under the normal system operation condition. Then this covariance provides a basis for the selection of forgetting factors. The estimates should be prevented from being impetuous, as well as from being indifferent to the changes shown in the measurements. A technique suggested in Ref. 19 amounts to the selection of forgetting factors that would force the adjusted covariance in Eq. (25) to stay within some prescribed bounds,

$$\sigma_{\min} I \le P_{k+1|k}^{\xi} \le \sigma_{\max} I \quad (38)$$

where $\sigma_{\min}$ and $\sigma_{\max}$ are positive constants, with $0 < \sigma_{\min} < \sigma_{\max} < \infty$, and I is the identity matrix. Let the dyadic expansion of $P_{k|k}^{\xi}$ be given by

$$P_{k|k}^{\xi} = \sum_{i=1}^{n_u} \alpha_{k|k}^i \boldsymbol{e}_k^i \left(\boldsymbol{e}_k^i \right)^T \quad (39)$$

where $\alpha_{k|k}^1, \ldots, \alpha_{k|k}^{n_u}$ are the eigenvalues of $P_{k|k}^{\xi}$, with $\alpha_{k|k}^1 \ge \cdots \ge \alpha_{k|k}^{n_u}$, and $\boldsymbol{e}_k^1, \ldots, \boldsymbol{e}_k^{n_u}$ are the corresponding eigenvectors, with $\|\boldsymbol{e}_k^1\| = \cdots = \|\boldsymbol{e}_k^{n_u}\| = 1$. Equation (39) can then be expressed as

$$P_{k+1|k}^{\xi} = \sum_{i=1}^{n_u} \frac{\alpha_{k|k}^i}{\lambda_k^i} \boldsymbol{e}_k^i \left(\boldsymbol{e}_k^i \right)^T + Q_k^{\xi}, \qquad 0 < \lambda_k^i \le 1$$

Following the argument in Ref. 19, the forgetting factor λ_k^i can be chosen as a decreasing function of the amount of the information received in the direction $\boldsymbol{e}_k^i$. Because eigenvalue $\alpha_{k|k}^i$ of $P_{k|k}^{\xi}$ is a measure of the uncertainty in the direction of $\boldsymbol{e}_k^i$, a choice of forgetting factor λ_k^i based on the preceding constraints can be

$$\lambda_k^i = \begin{cases} \lambda_0, & \alpha_{k|k}^i > \alpha_{\max} \\ \alpha_{k|k}^i \left\{ \alpha_{\min} + [(\alpha_{\max} - \alpha_{\min})/\alpha_{\max}] \alpha_{k|k}^i \right\}^{-1}, & \alpha_{k|k}^i \le \alpha_{\max} \end{cases} \quad (40)$$

The estimation algorithm will be applied to a HiMAT vehicle in the next section.

Control of HiMAT Vehicle

In this section, the robust LPV control synthesis methodology discussed in the preceding section is applied to control a HiMAT vehicle for possible actuator failures. It is assumed that only one of actuators may fail at a time. This implies that control reconfigurability of the HiMAT vehicle is never lost.[20] We do not know, however, which actuator fails, when it fails, and how severe is the failure. The system variations due to actuator failures can be modeled as an LFT–LPV system scheduled by a function of the estimated fault parameters. Parameter estimation errors can be aggregated into the system uncertainty description.

LFT–LPV Model of HiMAT Vehicle

The model of the HiMAT vehicle taken from the μ-synthesis toolbox[21] has two inputs, elevons δ_e and canards δ_c; two outputs, angle of attack α in radians and pitch angle θ in radians; and four states, velocity V in feet per second, angle of attack α, pitch rate q in radians per second, and pitch angle θ. The open-loop model is

$$\begin{bmatrix} \dot{x} \\ y \end{bmatrix} = \begin{bmatrix} A & B \\ C & 0 \end{bmatrix} \begin{bmatrix} x \\ u \end{bmatrix}, \qquad u = \begin{bmatrix} \delta_e \\ \delta_c \end{bmatrix} \quad (41)$$

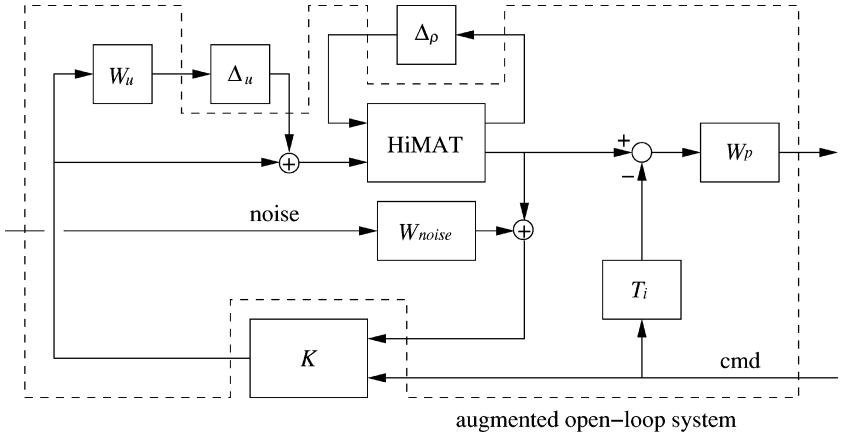

Fig. 3 Interconnection structure for the model matching problem.

where

$$A = \begin{bmatrix} -0.0226 & -36.6 & -18.9 & -32.1 \\ 0 & -1.9 & 0.98 & 0 \\ 0.012 & -11.7 & -2.63 & 0 \\ 0 & 0 & 1 & 0 \end{bmatrix} \tag{42}$$

$$B = \begin{bmatrix} 0 & 0 \\ -0.414 & 0 \\ -77.8 & 22.4 \\ 0 & 0 \end{bmatrix}, \qquad C = \begin{bmatrix} 0 & 1 & 0 & 0 \\ 0 & 0 & 0 & 1 \end{bmatrix} \tag{43}$$

To include possible actuator failures (loss of actuator effectiveness) in the model, fault parameters $0 \le \tau_1 \le 1$ and $0 \le \tau_2 \le 1$ are introduced for elevon and canard actuator, respectively. The state-space model in Eq. (41) is rewritten as

$$\dot{x} = Ax + [b_1\tau_1 \quad b_2\tau_2]u, \qquad y = Cx \tag{44}$$

where b_1 and b_2 are the columns of the matrix B defined in Eq. (43). The fault parameters are estimated using the parameter estimation algorithm described in the preceding section with bounded estimation error. In Eq. (44), $\tau_1 = 1 + \xi^1$ and $\tau_2 = 1 + \xi^2$, where the control effectiveness factors ξ^1 and ξ^2 are defined in the preceding section. Rewrite the fault parameters as

$$\tau_1 = \bar{\tau}_1 + \delta_1\, \mathrm{d}\tau_1, \qquad \tau_2 = \bar{\tau}_2 + \delta_2\, \mathrm{d}\tau_2 \tag{45}$$

where the magnitudes of error $\mathrm{d}\tau_1$ and $\mathrm{d}\tau_2$ are set as 0.1 and 0.1, respectively, and the real parameters δ_1 and δ_2 can independently vary from -1 to 1. The LFT–LPV model of the HiMAT vehicle is

$$\dot{x} = Ax + B\begin{bmatrix} \bar{\tau}_1 & 0 \\ 0 & \bar{\tau}_2 \end{bmatrix} u + B\begin{bmatrix} \mathrm{d}\tau_1 & 0 \\ 0 & \mathrm{d}\tau_2 \end{bmatrix} d_\Delta \tag{46}$$

$$e_\Delta = u, \qquad y = Cx \tag{47}$$

$$d_\Delta = \Delta_\rho e_\Delta, \qquad \Delta_\rho = \begin{bmatrix} \delta_1 & 0 \\ 0 & \delta_2 \end{bmatrix} \tag{48}$$

Although the LFT–LPV model in Eq. (46) is affine in the estimated fault parameter vector $\bar{\tau} = [\bar{\tau}_1 \;\; \bar{\tau}_2]^T$, the vector $\bar{\tau}$ cannot be chosen as an estimated scheduling parameter vector for LPV control synthesis because it would have included simultaneous actuator failures and would have led to unnecessarily conservative designs. To formalize correctly the single actuator failure assumption, an estimated scheduling parameter $\bar{\rho}$ is introduced, which ranges over $0 \le \bar{\rho} \le 2$,

$$\begin{aligned} 0 \le \bar{\rho} < 1: &\qquad 0 \le \bar{\tau}_1 < 1, \qquad \bar{\tau}_2 = 1 \\ \bar{\rho} = 1: &\qquad \bar{\tau}_1 = 1, \qquad \bar{\tau}_2 = 1 \\ 1 < \bar{\rho} \le 2: &\qquad \bar{\tau}_1 = 1, \qquad 0 \le \bar{\tau}_2 < 1 \end{aligned} \tag{49}$$

Note that the LPV model of the HiMAT vehicle is no longer affine in the estimated parameter $\bar{\rho}$.

LPV Controller Design

The control objective is to track a pitch angle command under possible actuator failures. A desirable controller should robustly stabilize the HiMAT vehicle over the prescribed range in Eq. (49) for the fault parameters. The controller synthesis problem is formulated as a model matching problem as shown in Fig. 3.

The ideal response model T_i of pitch angle is taken from the example in μ-synthesis toolbox.[21] The performance weighting function W_p and unmodeled dynamics W_u are also taken from the example in μ-synthesis toolbox.[21] The sensor noise is modeled as white noise with 0.6-deg amplitude for angle of attack and pitch angle measurements. The weighting functions in Fig. 3 are

$$T_i = \frac{1}{s/0.8 + 1}, \qquad W_p = 40\frac{s/50 + 1}{s/0.05 + 1}$$

$$W_u = 0.2\frac{s/5 + 1}{s/1000 + 1} I_2, \qquad W_{\text{noise}} = 0.01 I_2 \tag{50}$$

The uncertainty block Δ_u in Fig. 3 is diag($[\Delta_1, \Delta_2]$) where complex parameters $|\Delta_1| \le 1$ and $|\Delta_2| \le 1$ are associated with the unmodeled dynamics on elevon and canard channels, respectively. The uncertainty block Δ_ρ in Fig. 3 is defined as Eq. (48).

The control synthesis problem of the HiMAT vehicle is formulated to minimize the induced-$\mathcal{L}_2$ norm of the augmented LPV system with these weighting functions. To synthesize an LPV controller for the augmented open-loop system shown in Fig. 3, basis functions for $X(\bar{\rho})$ and $Y(\bar{\rho})$ are required in Eq. (10). The matrices $X(\bar{\rho})$ and $Y(\bar{\rho})$ are written as

$$X(\bar{\rho}) = \sum_i f_i(\bar{\rho}) X_i, \qquad X_i \in \mathcal{R}^{n\times n}$$

$$Y(\bar{\rho}) = \sum_j g_j(\bar{\rho}) Y_j, \qquad Y_j \in \mathcal{R}^{n\times n} \tag{51}$$

where basis functions $f_i(\bar{\rho})$ and $g_j(\bar{\rho})$ are selected before solving the LMI optimization in Eq. (10) for X_i and Y_j. There is no rigorous theoretical basis for choosing a minimal number of optimal basis functions for X and Y in general. Here, the basis function set is chosen to be $\{1, 1/(\bar{\rho} + 0.01), \bar{\rho}\}$ for X and Y to help the LMI optimization for total failure of either actuator ($\bar{\rho} = 0$ or $\bar{\rho} = 2$). Such a basis set renders adequate sensitivity of unknown matrices X_i and Y_j to all failure cases of interest. Note that it is not necessary to set $g_j(\bar{\rho})$ equal to $f_i(\bar{\rho})$.

A parameter rate bound needs to be specified to solve the LMI optimization in Eq. (10). To accommodate possibly sudden variation of the scheduling parameter in the case of an abrupt actuator failure, the parameter rate bound is set at a sufficiently large number

Table 1 LMI optimization in Eq. (10) γ values

Iteration	γ	S
1	1.23	diag([1,1,1,1])
2	0.71	diag([0.497, 0.168, 1.186, 1.277])
3	0.60	diag([1.404, 1.289, 1.801, 1.453])
4	0.54	diag([1.580, 2.193, 2.100, 1.187])
5	0.85	diag([2.007, 1.430, 2.506, 1.849])

$|\dot{\bar{\rho}}| < 100$. With the tractability of the LMI optimization in mind, the LMI constraints are evaluated at the following grid points:

$$\bar{\rho} \in \{\bar{\rho} | 0, 0.1, 0.2, \ldots, 1.9, 2\}$$

Also, the same grid points are used to solve the LMI optimization in Eq. (17). Because the matrix P is related with X and Y (Refs. 6 and 16), the basis function set for P is chosen as $\{1, 1/(\bar{\rho} + 0.01), \bar{\rho}\}$ as well.

In this paper, the scaling factor S is assumed to be constant independent of the scheduling parameter. The γ values and the corresponding scaling factor S for each iteration are given in Table 1. The scaling factor S is associated with the uncertainty block Δ given by

$$\Delta = \text{diag}([\Delta_\rho, \Delta_u]) \tag{52}$$

where Δ_ρ is defined in Eq. (48) and the uncertainty block Δ_u in Fig. 3 is associated with the unmodeled dynamics.

With use of the robust LPV synthesis methodology described in the second section, an LPV controller is designed for the HiMAT vehicle. Table 1 indicates that the iteration process is stopped at the fifth iteration because the γ value at the iteration is greater than the previous iteration. Recall that the iteration process is not guaranteed to be convergent. The performance index γ in the LMI optimization of Eq. (10) is significantly reduced from 1.23 to 0.54 as the iterations proceed. In the remainder of this paper, the LPV controller for the HiMAT vehicle designed at the fourth iteration step is used.

Simulations

In this section, the designed LPV controller is applied to control the HiMAT vehicle for predefined failure scenarios. One of the failure scenarios is that a total canard failure occurs between 1 and 10 s and a total elevon failure occurs between 20 and 40 s. The scheduling parameter, in seconds, corresponding to the failure scenario is

$$\rho = \begin{cases} 2.00, & 1 \le t < 10 \\ 1.00, & 0 \le t < 1 \quad 10 \le t \le 20 \\ 0.01, & 20 < t \le 40 \end{cases} \tag{53}$$

In the failure case, the pitch angle commands are given as 10 deg at 1 s, 0 deg at 10 s, and 10 deg at 20 s, sequentially.

For the purpose of comparison, a H_∞ controller is designed as a baseline controller that achieves the desired performance level at the healthy condition. In the design procedure of the H_∞ controller, the weighting functions defined in the fourth section are used. Note that the H_∞ controller cannot be scheduled for the faults. The closed-loop responses with this H_∞ controller are also simulated for the actuator failure scenario of Eq. (53) and are shown in Fig. 4. It can be seen that the H_∞ controller can achieve the desired performance level when canard fails($1 \le t < 10$ s). The H_∞ controller cannot, however, achieve the desired performance level at the elevon failure. This is consistent with the finding through reconfigurability calculation[20] that the canards are less effective in controlling the pitch movement than elevons and that loss of elevon effectiveness can significantly affect tracking the pitch commands. Also observe from Fig. 4 that the elevon signals of the H_∞ controller are significant despite the failure of the elevons. This implies that a reliable reconfigurable FTC law is required to keep elevon signals close to zero for elevon failure.

For the purpose of comparison, the LPV controller for the HiMAT vehicle is simulated both with and without actuator failures, and the simulation results are shown in Fig. 5. In this simulation, the

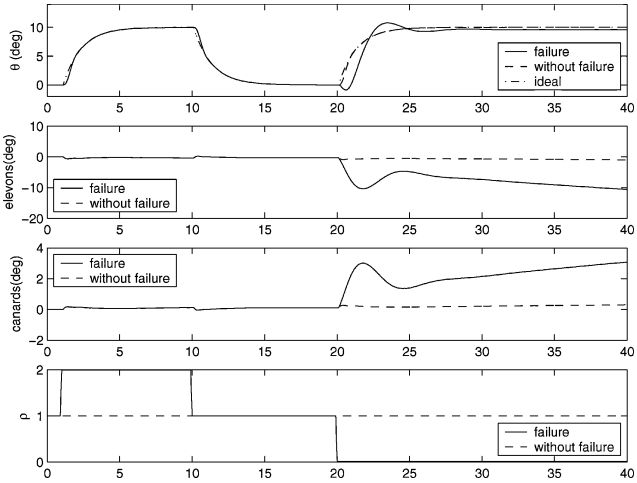

Fig. 4 H_∞ control simulations with and without actuator failures.

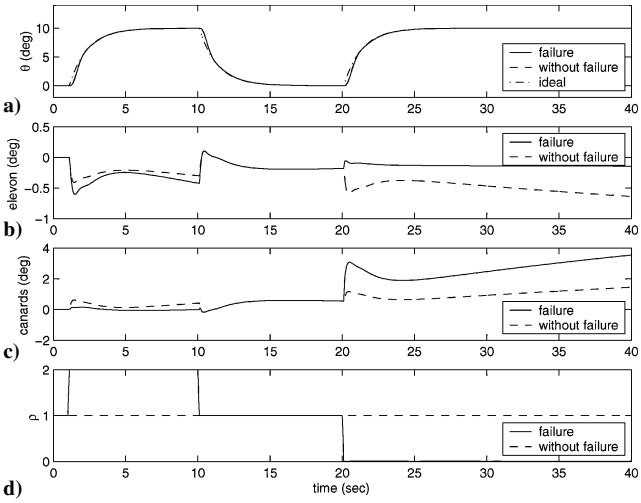

Fig. 5 LPV controller simulations with and without actuator failures.

FDI module is assumed to be perfect and estimates fault parameters without estimation errors. Under this assumption, the estimated scheduling parameter corresponding to the true failure parameters (Fig. 5d), is fed into the LPV controller. It is observed that the LPV controller achieves the desired goal of tracking pitch commands in the presence of actuator failures. It can be seen from Figs. 5b and 5c that the LPV controller always relies on the healthy actuator to track the pitch commands and abandons the failed actuator. For example, the LPV controller keeps the elevon actuator signals close to zero at the elevon actuator failure case.

Now, the fault parameters are estimated with an online estimator that is integrated into the LPV controller as shown in Fig. 1. The FDI module has two parts: One is the online estimator, which estimates fault parameters $\bar{\tau}_1$ and $\bar{\tau}_2$ using the two-stage adaptive Kalman filter, and the other carries out a simple logic that converts the failure estimates to the corresponding scheduling parameter estimate. The simple logic of Eq. (49) is modified because both the estimated fault parameters $\bar{\tau}_1$ and $\bar{\tau}_2$ can be less than one simultaneously before the fault parameter values are converged. The simple logic used in the simulation is

$$\bar{\tau}_1 \le \bar{\tau}_2 \Rightarrow \bar{\rho} \equiv 2 - \bar{\tau}_1, \qquad \bar{\tau}_1 > \bar{\tau}_2 \Rightarrow \bar{\rho} \equiv \bar{\tau}_2 \tag{54}$$

Recall that the estimated failure parameters $\bar{\tau}_1$ and $\bar{\tau}_2$ can vary only from 0 to 1, respectively, based on actuator faults.

The following set of parameter values are used in the two-stage adaptive Kalman filter. Sampling period T_s is set at 0.01 s to capture the response details of the open-loop dynamics of the vehicle. The

Table 2 Different sets of the varying forgetting factors

Case	λ_0	$\alpha_{\min}$	$\alpha_{\max}$
1	0.90	10	100
2	0.95	10	100
3	1.00	10	100
4	1.00	10^6	10^7

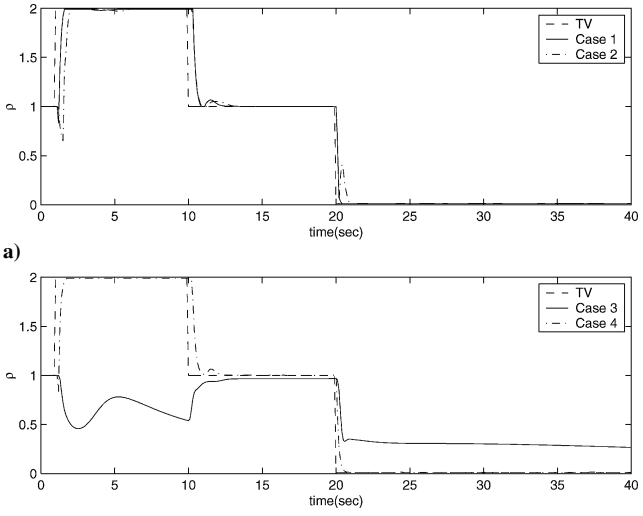

Fig. 6 Scheduling parameter estimates for cases in Table 2.

covariance matrices Q_k^x, Q_k^ξ, and R_k^ξ described in the third section are set as constant matrices with values

$$Q_k^x = 3\text{diag}([1, 0.01^2, 0.01^2, 0.01^2])$$

$$Q_k^\xi = 3\text{diag}([0.05^2, 0.05^2])$$

$$R_k^\xi = 3\text{diag}([0.01^2, 0.01^2])$$

The covariance matrices affect the convergence of the estimator and the noise level considered in the control synthesis in the fourth section. The initial values of estimated states $\hat{x}_{0|0}$ and effectiveness factors $\hat{\boldsymbol{\xi}}_{0|0}$ are set as $[0\ 0\ 0\ 0]^T$ and $[0\ 0]^T$, respectively. The initial covariance matrices $P_{0|0}^\xi$ and $\tilde{P}_{0|0}^x$ are set as $10I_2$ and $10I_4$, respectively. It is found that the estimates are sensitive to the selection of its initial values but insensitive to the selection of its initial error covariances. The most delicate part of the estimation lies with the selection of values for λ_0, $\alpha_{\min}$, and $\alpha_{\max}$ in Eq. (40). This is done by experiments and with little theoretical guidance. Different sets of values in Table 2 have been attempted.

The fault parameter online estimate results are shown in Fig. 6. It is obvious that the estimation results vary in different cases studied. From Fig. 6a, notice the value of λ_0 effect on convergence rate of estimation. When λ_0 is set at 1 in case 3 (Table 2), the effectiveness factor estimate is not convergent in the canard failure situation. For this case, the two fault parameter estimates are strongly coupled, which can cause false identification of faults. In cases 1, 2, and 4, initial transients in estimates are visible because the canards are less effective in controlling pitch angle. It is unknown how the control surface effectiveness is directly related with the transient behavior of the parameter estimator of the two-stage adaptive Kalman filter. For case 4, the covariance matrix P^ξ is immediately a high value after one step integration because $\alpha_{\min}$ is defined as 10^6. It is founded from the results of case 4 that the high value of the covariance matrix P_k^ξ leads to a good estimate of the scheduling parameter. However, it leads to very sensitive estimates for measurement noise. For further simulations, the parameter value set in case 1 is used in the two-stage adaptive Kalman filter.

The LPV controller is simulated with the online estimator using the parameter value set in case 1, and the simulation results are shown in Fig. 7. As shown in Fig. 7, the LPV controller is evaluated at the true values (TV) of the fault parameters and at the estimated fault parameters with a variable forgetting factor (VFF), respectively. Note that the LPV controller evaluated at the estimated parameter can achieve the desired performance of tracking the pitch commands. The difference in tracking performance between using the estimated parameter and the true parameter is very small at the steady state. The time delay and transient in the estimate has not been formalized in the LPV control synthesis process. The delay, though undesirable, is helpful in satisfying the rate bounds on the scheduling parameter, which is one of the assumptions of the LPV control synthesis methodology. Large delays in fault parameter estimates can be detrimental to the stability of a closed-loop system. This is a subject of future study.

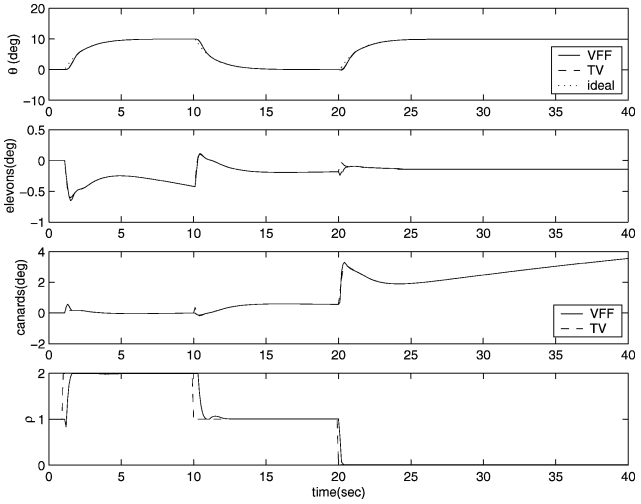

Fig. 7 Simulations with the online estimator.

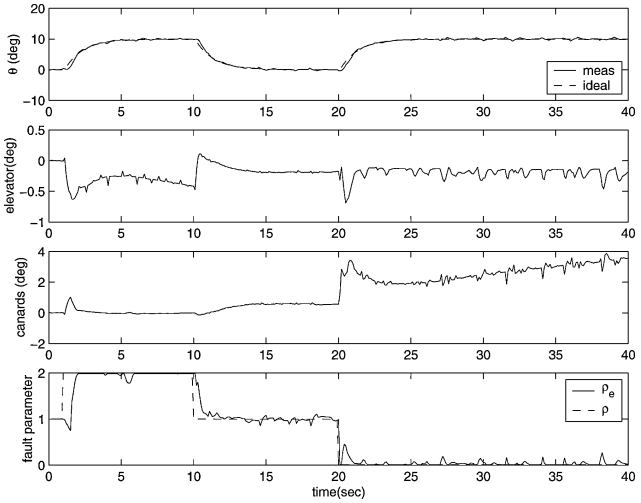

Fig. 8 Simulations with the online estimator with measurement noise.

The online estimator and the LPV controller are simulated with the measurement noise with the magnitude ± 0.01 rad of white noise used in control synthesis, and the simulation results are shown in Fig. 8. Observe that the LPV controller with the online estimator can stabilize the closed-loop system over the fault scenarios and achieve the desired performance level. Observe that the parameter estimation error in Fig. 8 is larger than 0.1 used in the LPV synthesis. It is an unknown dynamic coupling effect of the estimation between the controller and the FDI module. Note that it is still an open problem to characterize the coupling effect of the parameter estimator with the LPV control synthesis in robustness of measurement noise.

Conclusions

An LPV controller design problem based on an estimated scheduling parameter is formulated, and a proposed solution procedure is successfully applied to a pitch-axis flight control problem. The

system variations due to actuator failures are modeled as functions of estimated parameters, and the estimation errors are represented in an LFT form with an uncertainty block. An LPV controller synthesis problem with the estimation errors is transformed into two LMI optimizations, which are solved by an iteration method. The achieved performance level of the closed-loop system with the designed LPV controller is improved by introducing a constant scaling factor on the uncertainty block.

The iteration approach of the LPV synthesis methodology is applied to control the HiMAT vehicle subject to actuator failures. It is assumed that only one actuator can fail at a time. Actuator fault parameters of the HiMAT vehicle are estimated using the two-stage adaptive Kalman filter and are converted into the estimated scheduling parameter of the designed LPV controller. The LPV controller evaluated at the estimated fault parameter is simulated with the HiMAT vehicle and varies as true values of the fault parameter. The simulation results show that the LPV controller achieves the desired performance level when tracking pitch angle commands under actuator failures.

Acknowledgment

This research was supported in part by NASA under NASA Contract NAS1-02117 and in part by NASA under Cooperative Agreement NCC-1-02009 and is gratefully acknowledged by the authors.

References

[1]Belcastro, C., and Belcastro, C., "Applicaiton of Failure Detection, Identification, and Accommodation Methods for Improved Aircraft Safety," *Proceedings of American Control Conference*, American Automatic Control Council, Evanston, IL, 2001, pp. 2623–2624.

[2]Blanke, M., Izadi-Zamanabadi, R., Bogh, S. A., and Lunau, C. P., "Fault-Tolerant Control System—A Holistic View," *Control Engineering Control Practice*, Vol. 5, No. 5, 1997, pp. 693–702.

[3]Chen, J., Patton, R. J., and Chen, Z, "An LMI approach to Fault-Tolerant Control of Uncertain System," *Proceeding of the 1998 International Symposium on Intelligent Control*, Inst. of Electrical and Electronics Engineers, Piscataway, NJ, 1998, pp. 175–180.

[4]Ganguli, S., Marcos, A., and Balas, G., "Reconfigurable LPV Control Design for Boeing 747-100/200 Longitudinal Axis," *Proceedings of American Control Conference*, American Control Conference Council, Evanston, IL, 2002, pp. 3612–3617.

[5]Apkarian, P., and Adams, R., "Advanced Gain-Scheduling Techniques for Uncertain Systems," *IEEE Transactions on Control Systems Technology*, Vol. 6, No. 1, 1998, pp. 21–32.

[6]Wu, F., "Control of Linear Parameter Varying Systems," Ph.D. Dissertation, Dept. of Mechanical Engineering, Univ. of California, Berkeley, CA, Sept. 1995.

[7]Wu, F., Packard, A., and Balas, G., "LPV Control Design for Pitch-Axis Missile Autopilots," *Proceedings of the 34th IEEE Conference on Decision and Control*, Inst. of Electrical and Electronics Engineers, Piscataway, NJ, 1995, pp. 188–193.

[8]Shamma, J., "Gain-Scheduled Missile Autopilot Design Using Linear Parameter Varying Transformations," *Journal of Guidance, Control, and Dynamics*, Vol. 16, No. 2, 1993, pp. 256–261.

[9]Balas, G., Fialho, I., Packard, A., Renfrow, J., and Mullaney, C., "On the Design of LPV Controllers for the F-14 Aircraft Lateral-Directional Axis During Powered Approach," *Proceedings of the American Control Conference*, American Automatic Control Council, Evanston, IL, 1997, pp. 123–127.

[10]Balas, G., Ryan, J., Shin, J.-Y., and Garrard, W., "A New Technique for Design of Controllers for Turbofan Engines," AIAA Paper 98-3751, July 1998.

[11]Shin, J.-Y., "Worst-Case Analysis and Linear Parameter-Varying Gain-Scheduled Control of Aerospace Systems," Ph.D. Dissertation, Dept. of Aerospace Engineering and Mechanics, Univ. of Minnesota, Minneapolis, MN, Oct. 2000.

[12]Wu, N. E., Zhang, Y., and Zhou, K., "Detection, Estimation, and Accommodation of Loss of Control Effectiveness," *International Journal of Adaptive Control and Signal Processing*, Vol. 14, No. 7, 2000, pp. 775–795.

[13]Apkarian, P., and Tuan, H. D., "Robust Control via Concave Minimization Local and Global Algorithm," *IEEE Transactions on Automatic Control*, Vol. 45, No. 2, 2000, pp. 299–305.

[14]Belcastro, C., and Chang, B., "LFT Formulation for Multivariate Polynominal Problems," *Proceedings of American Control Conference*, American Control Conference Council, Evanston, IL, 1998, pp. 1002–1007.

[15]Zhou, K., Doyle, J., and Glover, K., *Robust and Optimal Control*, Prentice–Hall, Upper Saddle River, NJ, 1996, pp. 247–300.

[16]Becker, G., "Quadratic Stability and Performance of Linear Parameter Dependent Systems," Ph.D. Dissertation, Dept. of Mechanical Engineering, Univ. of California, Berkeley, CA, Sept. 1993.

[17]Dullerud, G. E., and Paganini, F., *A Course in Robust Control Theory*, Texts in Applied Mathematics, Springer, Berlin, 2000, Chap. 7.

[18]Keller, J. K., and Darouach, M., "Optimal Two-Stage Kalman Filter in the Presence of Random Bias," *Automatica*, Vol. 33, No. 9, 1997, pp. 1745–1748.

[19]Parkum, J. E., Poulsen, N. K., and Holst, J., "Recursive Foregetting Algorithms," *International Journal of Control*, Vol. 55, No. 1, 1992, pp. 109–128.

[20]Wu, N. E., Zhou, K., and Saloman, G., "Control Reconfigurability of Linear Time-Invariant Systems," *Automatica*, Vol. 36, No. 11, 2000, pp. 1767–1771.

[21]Balas, G., Doyle, J., Glover, K., and Packard, A., *μ Analysis and Synthesis Toolbox*, Mathworks, Natick, MA, 1995.